Journal of Coastal Research	SI	76	56–63	Coconut Creek, Florida	2016

Identifying Bathymetric Differences over Alaska's North Slope using a Satellite-derived Bathymetry Multi-temporal Approach

Shachak Pe'eri[†*], Brian Madore[†], John Nyberg[‡], Leland Snyder[‡], Christopher Parrish[§,+], and Shep Smith[‡]

[†]Center for Coastal and Ocean Mapping
University of New Hampshire
Durham, NH 03824, U.S.A.

[‡]National Oceanic and Atmospheric Administration/National Ocean Service
Marine Chart Division
Silver Spring, MD 20910, U.S.A.

[§]National Oceanic and Atmospheric Administration/National Ocean Service
National Geodetic Survey
Silver Spring, MD 20910, U.S.A.

[+]Civil & Construction Engineering
Oregon State University
Corvallis, OR 97331, U.S.A

www.cerf-jcr.org

www.JCRonline.org

ABSTRACT

Pe'eri, S.; Madore, B.; Nyberg, J.; Snyder, L.; Parrish, C., and Smith, S., 2016. Identifying bathymetric differences over Alaska's North Slope using a satellite-derived bathymetry multi-temporal approach. *In*: Brock, J.C.; Gesch, D.B.; Parrish, C.E.; Rogers, J.N., and Wright, C.W. (eds.), *Advances in Topobathymetric Mapping, Models, and Applications*. *Journal of Coastal Research*, Special Issue, No. 76, pp. 56–63. Coconut Creek (Florida), ISSN 0749-0208.

Many nautical charts of Alaska's North Slope are based on chart data that have not been updated since the early 1950s. Additionally, these charts may have been compiled using inadequate data and contain unsurveyed areas. However, with more days per year of diminished Arctic sea-ice coverage, including along the North Slope, marine transportation in this region has increased during the past decade, thus increasing the need for updated nautical charts. Due to limited resources available for U.S. Arctic surveying, the National Oceanic and Atmospheric Administration (NOAA) is evaluating the capabilities of satellite-derived bathymetry (SDB). This technology has proven useful as a reconnaissance tool in tropical and subtropical waters and clear-water conditions, especially over sandy seafloor. But in the Arctic, glacial flour from land reduces water clarity and limits the light penetration depth, which may affect SDB calculations. A new multi-temporal SDB approach is described in this paper using multiple images to extract "clear water" areas acquired on different dates. As a proof-of-concept, the extinction depth and bathymetry were calculated over areas that overlap with NOAA Charts 16081 and 16082 using Landsat 7 and Landsat 8 imagery. The derived and charted bathymetry are similar in most areas up to 4.5 m deep. The results of the study also identified a potential uncharted shoal. The multi-temporal SDB approach was further investigated by NOAA and was used to process imagery for other areas along Alaska's North Slope. As a result, the new editions of NOAA Chart 16081 include the location of a potential uncharted shoal, which is the first time an SDB product was utilized for a NOAA chart.

ADDITIONAL INDEX WORDS: *Arctic, navigation charts, satellite-derived bathymetry, water clarity*.

INTRODUCTION

Nautical Chart of Alaska North Slope

Most of the U.S. nautical charts that cover the Alaska North Slope have not been updated since the early 1950s (Table 1; Figure 1). An out-of-date chart infrastructure poses a challenge, especially as destinational ship transportation (*e.g.*, energy, fishing, and transit between communities) in the U.S. Arctic has increased recently (CMTS, 2013). In addition to the increase in Arctic marine traffic overall, there is some interest in using the waters along Alaska's North Slope as a route connecting the Atlantic and the Pacific Oceans through the Canadian Arctic Archipelago, known as the "Northwest Passage." Currently, the survey data used to compile NOAA charts are inadequate or nonexistent in much of the U.S. Arctic (NOAA, 2015). According to NOAA's U.S. Coast Pilot 9, much of the Bering Sea area is "only partially surveyed, and the charts must not be relied upon too closely, especially near shore" (NOAA, 2013, p. 7).

NOAA's Marine Chart Division (MCD) in the Office of Coast Survey compiles and updates nautical charts for all U.S. national waters in printable (Raster Nautical Charts) and vector (Electronic Navigational Charts) formats. The production and update of nautical charts depends on the availability of data, such as hydrographic surveys, shoreline data, tide measurements, and information pertinent to marine navigation. The vessel traffic along Alaska's North Slope contains boats operated by the local population, ranging from single person kayaks to industrially manufactured, aluminum boats; tankers and cruise ships used for maritime activity related to energy development, mining, tourism, and commercial shipping; and U.S. Coast Guard icebreakers used for security and scientific

DOI: 10.2112/SI76-006 received 19 February 2015; accepted in revision 23 August 2015.
*Corresponding author: Shachak@ccom.unh.edu

research (CMTS, 2013). Depths that are generally regarded as significant to various types of marine navigation can reach up to 40 m (IHO, 2008). But in the Arctic, there have not been many charts produced or updated due to the logistical challenges and the short survey period during the summer season. In fact, only a few surveys over the past 70 years have been conducted in the mid-water depths (most of which are between 40 and 200 m).

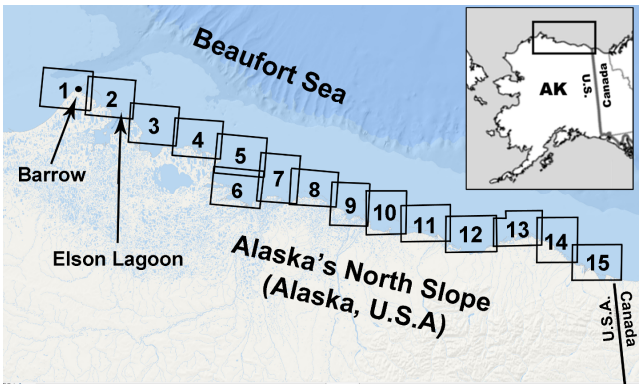

Figure 1. NOAA nautical charts over the Alaska North Slope. NOAA chart number, scale, and additional data are provided in Table 1 using the chart index numbers in the figure.

Table 1. *Current NOAA nautical charts available over Alaska's North Slope. The index numbers refer to the chart coverage areas presented in Figure 1. The last hydrographic survey refers to the most recent survey that was conducted within the area covered by the NOAA chart.*

Index #	Chart	Scale	Name	Last Hydrographic Survey
1	16082	1:47,943	Pt. Barrow and Vicinity	1951
2	16081	1:48,149	Scott Pt. and Tangent Pt.	1952
3	16067	1:48,767	Approaches to Smith Bay	1952
4	16066	1:48,973	Pitt Pt. and and Vicinity	1953
5	16065	1:49,177	Cape Halkett and Vicinity	1953
6	16064	1:49,794	Harrison Bay – Western Part	1953
7	16063	1:49,590	Harrison Bay – Eastern Part	1953
8	16062	1:49,794	Jones Island and Approaches	1951
9	16061	1:50,000	Prudhoe Bay and Vicinity	1951
10	16046	1:50,204	McClure and Stockton Islands and Vicinity	1950
11	16045	1:50,615	Brullen Pt. and Brownlow Pt.	1950
12	16044	1:50,819	Camden Bay and Approaches	1950
13	16043	1:50,819	Barter Island and Approaches	1952
14	16042	1:51,024	Griffin Island and Approaches	1952
15	16041	1:51,639	Demarcation Bay and Approaches	1952

The only recent attempt was conducted in 2013 around Point Barrow, Alaska. The NOAA 2013 survey was a local, partial bottom coverage that was mainly to detect changes in the bathymetry in the 10 to 50 m depth ranges.

The U.S. Committee on Marine Transportation System report and the Implementation Plan for The National Strategy for the Arctic Region state that the infrastructure that supports safety, environmental protection, and commercial efficiency must be enhanced (CMTS, 2013; White House, 2014). Based on increasing interest of the U.S. government in the Arctic, NOAA recently published a charting plan for sustainable marine transportation in Arctic Alaska (NOAA, 2013). Modern updated nautical charts at an appropriate scale can provide the foundation for improved transportation safety in the area. As part of a periodic review conducted by NOAA's MCD for 2014–2015, Arctic charts are now being evaluated for survey planning and prioritization.

A potential resource for chart evaluation is multispectral satellite imagery, which provides repeatable coverage of remote areas that are hard to access. Satellite-derived bathymetry (SDB) has proved to be a useful reconnaissance tool in tropical and subtropical regions with clear water conditions, especially over a sandy bottom (Pe'eri *et al.*, 2014; Philpot *et al.*, 2004; Stumpf, Holderied, and Sinclair, 2003). However, it is very difficult to extract good information over the Arctic marine areas using a single satellite image. Land-based glacial powder that is composed of silt and clay particles scatters and attenuates the sunlight in the water and is one of the major environmental factors that limit the light penetration depth. The long settling times of the glacial powder in the water can be on the order of days (Folk, 1980). The turbid waters along the coastline are highly variable, both spatially and temporally. Other recent studies suggest using infrared (IR) satellite imagery to map shoals based on the Arctic ice cover on the water surface that does not retreat uniformly (Nghiem *et al.*, 2012; Nghiem, Van Woert, and Neumann, 2015). Ice-cover patterns that occur during melting periods depend on climate change and seafloor morphology. IR imagery can be used to discriminate between deep-water areas along the shoreline (*e.g.,* channels) with no sea-ice cover and shallow-water areas (*e.g.*, shoals) that remain covered by ice. However, it is not possible to determine changes in depth from IR imagery because the extent of ice cover also depends on the local currents and water temperature, which can vary spatially and temporally.

In this study, a multi-temporal SDB approach was developed to evaluate NOAA's Arctic charts using Landsat imagery. The overarching objective was to obtain quantifiable information on the bathymetric differences since the last hydrographic survey was charted. The modified SDB approach presented in this study compiles multiple satellite images over a 15-year period to extract only areas that show minimum depth changes between two satellite images as an indication of clear waters. The procedure is based on the assumption that the temporal variability in water column turbidity in the Arctic is greater than changes in seafloor morphology over the 15-year period, which would enable NOAA to detect changes from the charted data. Although suspended matter can travel fast, on the order of hours,

from the mouth of a river or inlet to a certain location along the shoreline, coastal erosion or accretion (excluding major weather events) is on the order of days to years (Davis and Fitzgerald, 2014). Bathymetry of the North Slope was generated using Landsat 7 imagery from 1999–2002 and Landsat 8 imagery from 2013–2014. Hydrographic survey soundings from charts 16081 and 16082, referred to as "depth soundings," were used to reference the SDB models to chart datum.

Alaska's North Slope

Alaska's North Slope in this study is defined as the coastal area along the Beaufort Sea, a marginal sea of the Arctic Ocean (Figure 1). The field season along Alaska's North Slope is short, and survey work in this region is labor-intensive, logistically difficult, and expensive (Paine *et al.*, 2013). In addition to limited transit infrastructure that includes very few roads and a severely restricted off-road access, the environmental conditions are considered harsh (NAP, 2003). The ground temperatures range from 5 to 15 °C in the summer and -18 °C to -40 °C in the winter. Offshore, the sea-ice cover begins to retreat toward the summer and upwelling of warm waters from the Pacific Ocean enhances the melting of the ice cover (Carmack and Chapman, 2003). However, the ocean surface begins to freeze again around September–October (Nghiem and Newmann, 2007).

The most northern part of Alaska's North Slope was selected as a study site (Figure 2). This area overlaps with NOAA Chart 16081 and 16082 from latitudes 71˚05'N to 71˚29' and longitudes 154˚50' to 157˚25' (Figure 2). The hydrographic surveys that were used to compile the chart were conducted from 1945 to 1951. The coastal area between Point Barrow in the west and Dease Inlet in the east is characterized as flat with no wind barriers. The sun does not rise above the horizon at Barrow, Alaska, from November 18 to January 24. Each summer, a shallow surface layer (from 0.2 m to more than 2 m in thickness) of the permafrost terrain layer thaws (NAP, 2003). The meltwater of this layer cannot filter downward through the underlying impervious permafrost, causing runoff, erosion, and soil flowage. Thus, the near-shore waters are turbid from glacial powder and sediment from surface geology that includes shale, sandstone, graywacke, siltstone, and conglomerate (Molenaar, Bird, and Collett, 1986). The water turbidity is varied spatially and temporally according to local currents and runoff conditions. As a result, light penetration through the water column is not uniform and typically limited to a few meters in depth.

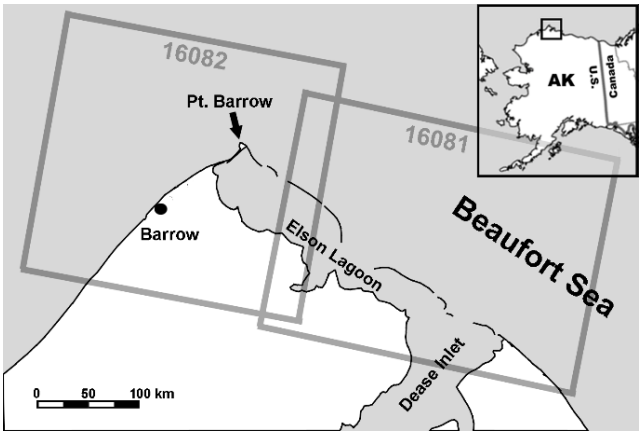

Figure 2. Geographic settings of the study site. The gray boxes mark the areas presented in NOAA Charts 16081 and 16082.

SATELLITE-DERIVED BATHYMETRY SINGLE-IMAGE APPROACH

Current and historical Landsat imagery is available to the general public at no cost. Imagery from Landsat satellites is collected and archived by the U.S. Geological Survey and made available at http://earthexplorer.usgs.gov. The archive includes the current Landsat 8 that has been operational since 2013 and previous Landsat missions, such as Landsat 7 that was fully operational from 1999–2003. (After May 2003, Landsat 7 imagery is still available but with data gaps caused by the Scan-Line Corrector failure.) The swath width of Landsat 7 and Landsat 8 imagery is 185 km with an average ground resolution of about 28.5 m, which is sufficient for reconnaissance applications for charts at a scale smaller than 1:50,000 (Pe'eri *et al.*, 2014).

The SDB procedure provides a simple reconnaissance tool for hydrographic offices around the world. The procedure is already in commercial use and its steps are documented in public literature (IHO, 2013; Pe'eri *et al.*, 2014). The concept of single-image SDB began in the late 1970s (Lyzenga, 1978) and has since been investigated by international hydrographic offices (*e.g.*, the French Service de Hydrographique et Oceanographique de la Marine and the United Kingdom Hydrographic Office) for potential use as an operational tool.

The most common method used to derive bathymetry from satellite imagery is an optimization approach using band-ratio calculation (Philpot *et al.*, 2004; Stumpf, Holderied, and Sinclair, 2003). The optimization approach utilizes two bands at different wavelength ranges to reduce the number of parameters required to infer depth. The bottom radiance observed by each band will decay exponentially with depth (Jerlov, 1976). Assuming a uniform mixture in the water column and that each band maintains a near-constant attenuation value, the ratio of the bands is the difference of the diffuse attenuation coefficient between the two wavelength ranges (Dierssen *et al.*, 2003; Stumpf, Holderied, and Sinclair, 2003). As a result, the ratio of the logs of the two bands is expected to vary linearly with depth. The most common algorithm used in single-image SDB is the ratio of natural logs approach, typically between the blue and green bands (Stumpf, Holderied, and Sinclair, 2003):

$$z = m_1 \left(\frac{ln(\mathrm{L_{obs}}(\lambda_i))}{ln(\mathrm{L_{obs}}(\lambda_j))} \right) - m_0 \qquad (1)$$

where m_1 and m_0 are tunable constants to linearly transform (*i.e.*, scale and shift) the algorithm results in a charted depth. Control points that are selected from survey measurements within the chart enable the vertical referencing of the bathymetry to chart datum. There is no need to measure the tide height during the image acquisition, as differences in water levels are usually well

approximated as a vertical offset and do not impair the linear relationship between depth soundings and ratio algorithm output. The main limiting factor affecting the performance of satellite-derived bathymetry is water clarity. As a result, the water depth of the seafloor can only be estimated to the extent of light penetration. When using a single image approach, a plume of suspended matter in the water can be misinterpreted as a shoal, an area higher than its surroundings. Previous work has shown that sediment plumes produce "false bathymetry" areas that are different in depth than the actual bottom bathymetry (Pe'eri *et al.*, 2014; Philpot *et al.*, 2004; Stumpf, Holderied, and Sinclair, 2003). Because any changes that are observed in the bathymetry may be due to the turbidity in the water rather than the bottom, a potential solution is to use a multi-temporal approach to derive bathymetry from at least two satellite images over the same area at different times.

SATELLITE-DERIVED BATHYMETRY MULTI-TEMPORAL APPROACH

For this study, the SDB approach was revised to include multiple images in order to identify temporal changes of the water turbidity in the near-shore areas. If the turbidity is constantly changing between two satellite images acquired at different times, then inferred depths of the two images will vary as well. It is reasonable to assume that the contribution from the temporal variability in water-column turbidity to SDB models is greater than the temporal variability of the seafloor (Davis and Fitzgerald, 2014). This assumption forms the basis of a "clear-water" criterion in the multi-temporal SDB calculation, where similar depths inferred by at least two images over the same area represent bottom detection. If different depths are inferred between two images over the same area, then the detection is suspected as a false shoaling effect and the area is excluded from further analysis. The assumption underlying the clear-water criterion algorithm was tested using WorldView-2 (WV-2) imagery over Elson Lagoon, Alaska (Figure 3). Although the swath width of WV-2 (18 km) is much smaller than the swath width of Landsat 7 (185 km), the WV-2 image resolution (~2 m) provides the ability to identify smaller features that cannot be observed in the Landsat 7 imagery (28.5-m pixel resolution). Based on empirical testing using depth differences of two WV-2 images to hydrographic survey soundings, a 1% depth-difference threshold excluded depth differences greater than 4 m.

In order to test the clear-water criterion, the bathymetric models from the SDB approach were required to be on the same scale. Control points cannot be used to vertically reference each of the bathymetric models before clear-water criterion is applied because it is not possible to know if a control point is from an area that is bottom detection or false shoaling in the bathymetric model. In order to compare the SDB models to each other prior to vertical referencing, one SDB model was assigned as the reference and the other SDB model was matched using histogram equalization. This pre-processing step is supported by the assumption that cloud-free and ice-free satellite images with a large footprint (*e.g.*, for Landsat imagery 185 km swath width) observed the same land features. Accordingly, the histograms of all the pixel values in the image should have similar characteristics. Although the near-shore bathymetry and the turbidity along the coastline may change from one image to the next, the radiometric contribution will be small in a large-footprint image that covers large areas of the ocean.

The processing steps for the SDB multi-temporal procedure were revised as follows:

Pre-processing and initial bathymetry estimation. After downloading all the available satellite images over the study site (Elson Lagoon, AK), the same pre-processing (glint/cloud correction, land/water separation, and spatial filters) and bathymetry estimation steps used in the SDB single-image approach were applied to each of the images (Pe'eri *et al.*, 2014).

Histogram equalization. A histogram equalization was applied to all of the inferred bathymetry models. In order to conduct the histogram equalization in ArcMap, a simple stretch transform was used. An arbitrary dataset was assigned as a reference image. The population of the second image, $P(I_S)$, was equalized to the population distribution of the reference image, $P(I_M)$, using a 5% criterion:

$$P'(I_S) = P_{CI5}(I_M) + \left(\frac{P_{CI95}(I_M) + P_{CI5}(I_M)}{P_{CI95}(I_S) + P_{CI5}(I_S)} - P_{CI5}(I_S)\right) \cdot P(I_S) \quad (2)$$

where *CI5* and *CI95* are the 5% and 95% levels of confidence interval, respectively.

Identification of the clear-water areas. Difference maps were calculated between all available pairs of the bathymetry estimations. For example, four images will produce six pairs (difference maps) that can be used to identify clear-water areas. The values of the bathymetry estimation results using the blue/green band ratio algorithm (Equation 1) are close to 1.0. Turbid areas are masked out from the difference maps using a 1% threshold:

$$P(I_M) - P'_i(I_S) < 0.01 \quad (3.1)$$

$$P'_i(I_S) - P'_j(I_S) < 0.01 \quad (3.2)$$

where $P'_i(I_S)$ and $P'_j(I_S)$ are the slave images after histogram equalization ($i \neq j$).

Vertical referencing and compilation. The clear-water areas from all the pairs were compiled together using an averaging function in the overlapping areas. The compiled solution was vertically referenced to the chart datum using the same referencing steps in the SDB single-image approach; *i.e.*, a linear regression was calculated between the compiled clear-water areas to the depth soundings or depth collected from a recent hydrographic survey (Pe'eri *et al.*, 2014).

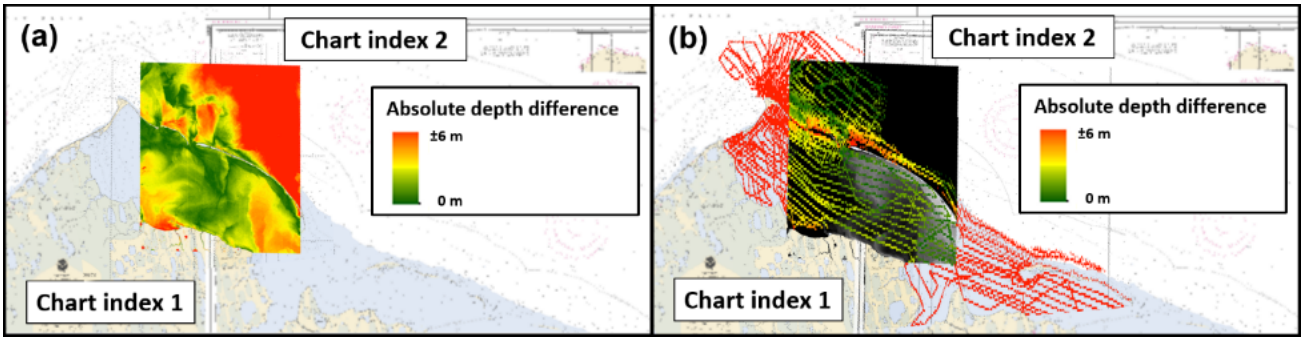

Figure 3. SDB results supporting the clear-water assumption: (a) depth difference between two WV-2 satellite images acquired at different times (July 21, 2010 and August 10, 2010), and (b) depth difference between WV-2 imagery (August 10, 2010) and hydrographic surveys soundings (1945 to 1951) that were used to compile NOAA Charts 16081 and 16082.

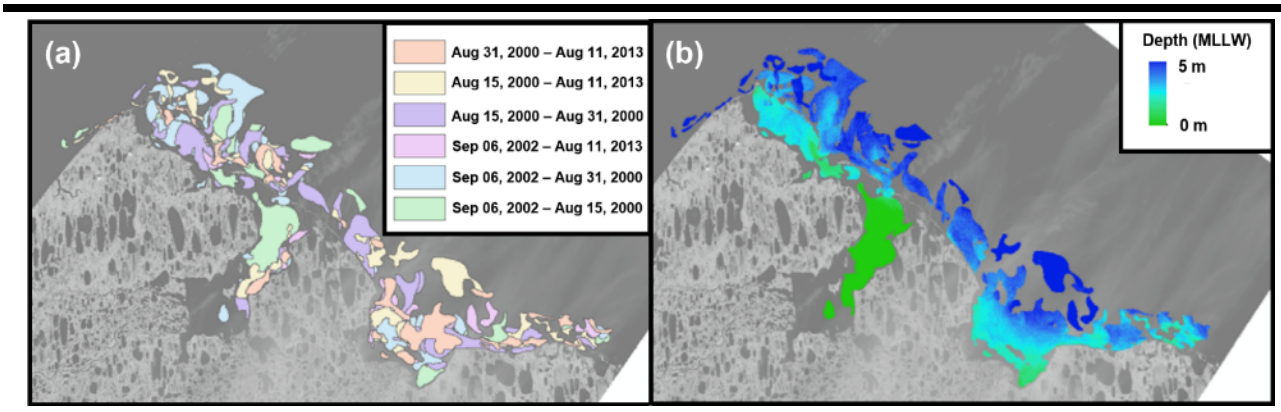

Figure 4. Multi-temporal SDB: (a) Polygons of the six pairs of clear-water areas were derived from four images. (b) The resulting bathymetry reference in meters to the MLLW chart datum.

RESULTS

As a proof-of-concept, the shallow-water bathymetry was derived over the western edge of the North Slope that extends from Elson Lagoon, Alaska, to Point Barrow, Alaska (Figure 2). Four Landsat images that overlapped with NOAA Charts 16081 (scale 1:48,149) and 16082 (scale 1:47,943) were processed to generate six pairs. The clear-water areas from each pair were extracted and the bathymetry models from all six pair were merged into one dataset using an averaging function in the overlapping areas (Figure 4a). The compiled solution was vertically referenced to the chart datum (Figure 4b). Although NOAA conducted a recent (2013) survey near Barrow, the survey lines were in deeper water and did not overlap the bathymetry-model areas. The horizontal datum for the Landsat imagery and the NOAA charts were transformed from North American Datum 1983 (World Geodetic System 1984 original; WGS-84), with a Mercator projection (scale 1:47,943 at latitude 71˚20') into WGS-84 geographic coordinates (Latitude, Longitude). The vertical datum of NOAA Charts 16081 and 16082 is Mean Lower Low Water (MLLW). Although the depth soundings were measured in feet, the depths were converted into meters in order to be consistent with MCD's Electronic Navigational Charts and international charting datasets.

Due to lack of recent survey data in the study area, the derived bathymetry was evaluated against the depth soundings from historical surveys. The calculated extinction depth ranges of the bathymetry models are between 4 and 6 m, depending on the acquisition date of the imagery. A comparison between the compiled results and the depth soundings showed a mean difference of 0.11 m with a standard deviation of 1.09 m (Figure 5). The largest differences were observed near the coastline (marked in a gray circle in Figure 5). This may be explained by changes of the coastline bathymetry, possibly caused by climate change, over the 70 years since the last hydrographic survey in the area (USACE, 2009).

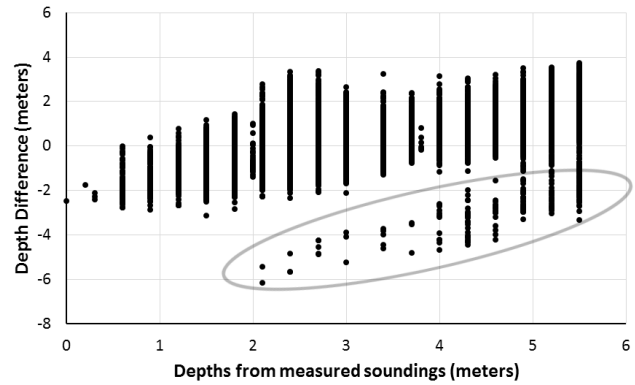

Figure 5. Scatterplot of depth differences between bathymetry derived using the multi-temporal SDB approach and the depth soundings. Depth differences that were outliers and that were identified along the coastline are marked in the gray circle.

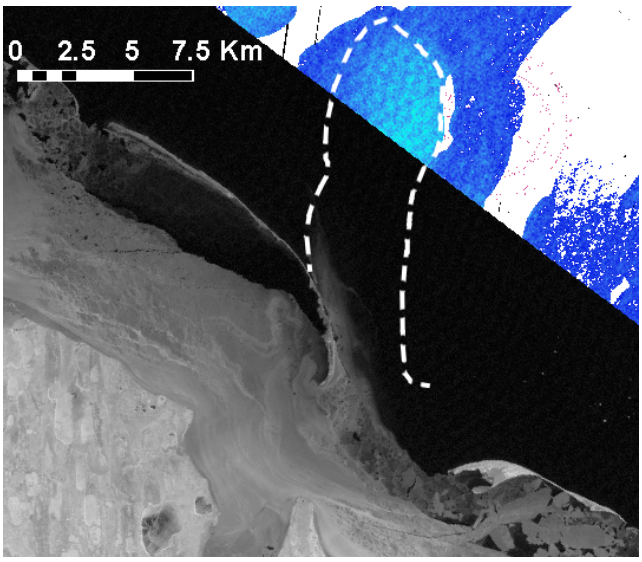

Figure 6. Landsat 7 infrared band (October 3, 2001) showing the sea-ice coverage overlaid on the multi-temporal SDB results. The extent of the uncharted shoal is marked with a dashed white line.

The bathymetry derived from the multi-temporal SDB matched most of the overlapping charted areas. A visual comparison between the multi-temporal SDB results and the chart also identified a shoal feature that was not marked on the chart, located on northeast of Elson Lagoon (Figure 6). The size of the suspected shoal is more than 3 km wide and 10 km long. The location of the shoal was also estimated based on a single-image SDB using WV-2 imagery and sea-ice coverage using Landsat 7 IR imagery. Only one WV-2 image (acquisition date: August 10, 2010) was available during the study that identified a larger shoal over the same location. The larger extent most likely is a plume of suspended matter in the water that surrounds the shoal. However, it was hard to separate the shoal from the surrounding suspended sediments. In addition, a sea-ice patch was observed overlapping the location of the suspected shoal using a Landsat 7 IR band image (Band 4; 770 to 900 nm) from October 3, 2001. The sea-ice patch was not parallel to the shoreline, and based on previous work conducted by Nghiem, Van Woert, and Neumann (2005) and Nghiem *et al.* (2012), the patch was an indicator of shoal areas (Figure 6).

DISCUSSION

The results of the multi-temporal SDB approach over the western part of Alaska's North Slope were considered successful. A shallow-water bathymetry area of 1,292 km^2 was inferred. Most of the overlapping areas between the current derived bathymetry (*i.e.*, 2000–2013) matched the charted bathymetry that was collected 70 years earlier, in the 1950s. The rest of the seafloor area in the chart was optically deep (*i.e.*, it was not possible to detect the bottom from satellite imagery) and was not evaluated. The SDB multi-temporal results extended beyond the boundaries of the historical surveys that compiled charts 16081 and 16082. The uncharted shoal that was identified using the multi-temporal SDB approach was reaffirmed in the ice-coverage maps using IR imagery. The performance of the multi-temporal SDB approach in this study was limited mainly because of available depth soundings and Landsat 7 imagery. The bathymetric model of Elson Lagoon was referenced using depth soundings that were collected between 1945 and 1951. Natural weather events or anthropogenic activities may have caused the near-shore sediments to shift over the years, which increased uncertainty in these areas. Another issue was the inherent systematic noise in the Landsat 7 green channel, which resulted in a "wave" artifact superimposed on the bathymetry. As a result, systematic noise in the bathymetry of 0.5 to 0.75 m in amplitude was observed on the SDB. A low pass filter was applied to the SDB bathymetry in order to remove this contribution to the bathymetry. As more Landsat 8 imagery will be available in the near future, it will be possible to re-process Alaska's North Slope using this more recent imagery.

A descriptive report on the multi-temporal SDB procedure and position data on the uncharted shoal were submitted to MCD at NOAA. As a result, the new editions of NOAA Chart 16081 (Raster chart and Electronic Navigational Chart) include the location of the potential uncharted shoal with a supplemental note and an illustration in the source diagram (Figure 7). This is the first time an SDB product was utilized for a NOAA chart. The multi-image approach has been adopted in MCD for further evaluation and to derive bathymetry for the rest of the Alaska North Slope (Figure 8). Details on the imagery used to derive bathymetry in six areas (Area A to Area F) are provided in Table 2. Both single-image and multi-temporal approaches to SDB are reconnaissance tools for investigation of coastal areas before a high-resolution hydrographic survey (*e.g.*, Multibeam Echosounder and Airborne Lidar Bathymetry) is conducted.

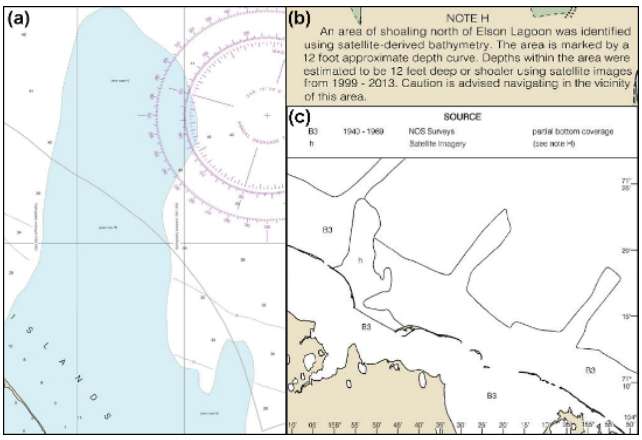

Figure 7. NOAA Raster Chart 16081 that includes a new shoal that was identified using multi-temporal SDB: (a) revised 12-foot contour marking the location of the new shoal, (b) chart note describing the method used to identify the shoal, and (c) source diagram.

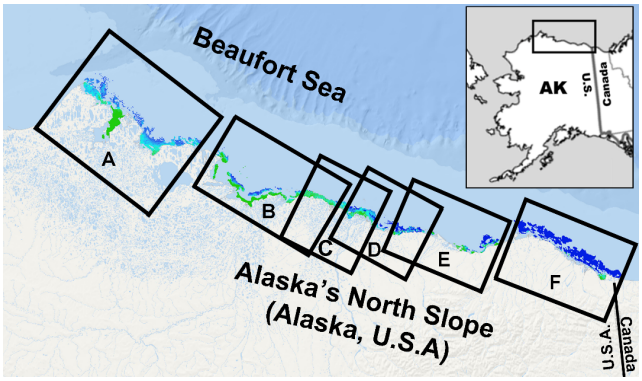

Figure 8. Bathymetry calculated for the whole Alaska's North Slope over six scenes. Details on the imagery used in these scenes is provided in Table 2.

Table 2. *Landsat imagery used to derive bathymetry over the Alaska's North Slope.*

Area	Date	Path	Row
A	August 15, 2000	79	10
	August 31, 2000	79	10
	September 06, 2002	79	10
	August 11, 2013	79	10
B	September 20, 2000	75	10
	July 21, 2013	76	10
C	September 20, 2000	75	10
	July 23, 2001	73	11
	July 17, 2002	74	10
	July 16, 2013	73	11
	August 01, 2013	73	11
D	July 27, 1999	72	11
	July 17, 2002	74	10
	August 10, 2013	72	11
E	August 05, 1999	71	11
	August 30, 2000	72	11
	August 10, 2013	72	11
	September 11, 2013	72	11
F	August 07, 1999	69	11
	September 06, 2013	69	11
	September 13	70	11
	October 15, 2013	70	11

CONCLUSIONS

A multi-image SDB approach was developed in order to evaluate charted near-shore bathymetry in the turbid and spatially and temporally varying waters of the North Slope of Alaska. The approach utilizes satellite imagery from multiple epochs over the same area in order to extract clear-water areas that are used to derive bathymetry. The key steps in the procedure include pre-processing and initial bathymetry estimation, histogram equalization, identification of the clear-water areas, vertical referencing, and compilation. The procedure was tested over the western edge of Alaska's North Slope as a proof-of-concept. Although the results can be further improved with a quantitative evaluation, bathymetry can be derived over non-uniform moderately turbid areas that allow bottom detection using the new SDB approach to evaluate chart adequacy. The main challenge to using the multi-temporal approach in remote areas is the vertical referencing of the bathymetric dataset due to lack of depth soundings that can be used as current control measurements. The number of soundings required in the procedure depends on the ability to create a linear relationship between the SDB algorithm and the water depth from the control measurements. This number may vary based on the survey quality and the distribution of the control measurements over different depth ranges. In addition, Landsat 7 imagery contained an unidentified systematic error that created a "wave" artifact in the bathymetry. It is recommended to remove the noise with post-processing filters or derive bathymetry using only Landsat 8 imagery. The study results and the multi-image approach have been adopted by NOAA's MCD for further evaluation.

ACKNOWLEDGMENTS

This project was partially funded from the UNH / NOAA Joint Hydrographic Center grant NA10NOS4000073. The authors want to thank LTJG Anthony Klemm, NOAA, for his thoughts and comments and NOAA for providing the bathymetric data from the nautical charts used for this study. Also, the authors would like to thank the anonymous reviewers for their comments that have improved the manuscript.

LITERATURE CITED

Carmack, E. and Chapman, D.C., 2003. Wind-driven shelf/basin exchange on an Arctic shelf: The joint roles of ice cover extent and shelf-break bathymetry. *Geophysical Research Letters,* 30(14), 1778.

Davis, R.A. and Fitzgerald, D.M., 2014. *Beaches and Coasts*. Malden, MA: Blackwell Publishing Company, 419p.

Dierssen, H.M.; Zimmerman R.C.; Leathers, R.A.; Downes, T. V., and Davis, C.O., 2003. Ocean color remote sensing of seagrass and bathymetry in the Bahamas Banks by high-resolution airborne imagery. *Limnology and Oceanography,* 48(1_part_2), 444–455.

Folk, R.L., 1980. *Petrology of Sedimentary Rocks*. Austin, TX: Hemphill Publishing Company, 182p.

International Hydrographic Organization (IHO), 2008. *IHO Standards for Hydrographic Surveys (5th edition)*. Monaco: International Hydrographic Bureau, 36p.

International Hydrographic Organization (IHO) - International Ocean Commision (IOC), 2013. *The IHO-IOC GEBCO Cook Book, Edition 11.1.13*. Monaco: International Hydrographic Office (IHO)/International Ocean Commission (IOC), *IHO Publication B-11 and IOC Manuals and Guides, 63*, p. 243–304.

Jerlov, N.G., 1976. *Marine Optics*. New York: Elsevier Scientific Publication, 230p.

Lyzenga, D.R., 1978. Passive remote sensing techniques for mapping water depth and bottom features. *Applied Optics*, 17(3), 379–383.

Molenaar, C.M.; Bird, K.J., and Collett, T.S., 1986. *Regional correlation sections across the North Slope of Alaska*. *U.S. Geological Survey Miscellaneous Field Studies, Map MF-1907*. 1 sheet.

National Academies Press (NAP), 2003. *Cumulative Environmental Effects of Oil and Gas Activities on Alaska's North Slope*. Washington, DC: The National Academies Press, 304p.

National Oceanic and Atmospheric Administration (NOAA), 2015. Bering Sea: Chart 16006. *In*: U.S. Coast Pilot 9, Alaska: Cape Spencer to Beaufort Sea (33rd Edition), Washington, DC, p. 395–397.

National Oceanic and Atmospheric Administration (NOAA), 2013. *Arctic Nautical Charting Plan – a plan to sustainable marine charting transportation in Alaska (Feb. 15, 2013)*. Silver Spring, MD: Office of Coast Survey, Marine Chart Division publication, 51p.

Nghiem, S.V.; Van Woert, M.L., and Neumann, G., 2005. Rapid formation of a sea ice barrier east of Svalbard. *Journal of Geophysical Research*, 110, C11013.

Nghiem, S.V. and Neumann, G., 2007. Arctic Sea-Ice Monitoring. *In*: *2007 McGraw-Hill Yearbook of Science and Technology*. New York: McGraw-Hill, pp. 12–15.

Nghiem, S.V.; Clemente-Colon, P.; Rigor, I.G.; Hall, D.K., and G. Neumann, 2012. Seafloor control on sea ice, Deep-Sea Research Deep Sea Research, Part II. *Topical Studies in Oceanography*, 77–80, 52–61.

Paine, J.G.; Andrews, J.R.; Saylam, K.; Tremblay, T.A.; Averett, A.R.; Caudle, T.L.; Meyer, T., and Young, M.H., 2013. Airborne lidar on the Alaskan North Slope: wetlands mapping, lake volumes, and permafrost features. *The Leading Edge*, 32(7), 798–805.

Pe'eri, S.; Parrish, C.; Azuike, C.; Alexander, L., and Armstrong, A., 2014. Satellite remote sensing as a reconnaissance tool for assessing nautical chart adequacy and completeness. *Marine Geodesy*, 37(3), 293–314.

Philpot, W.D.; Davis, C.O.; Bissett, W.P.; Mobley, C.D.; Kohler, D.D.R.; Lee, Z.; Bowles, J.; Steward, R.G.; Agrawal, Y.; Trowbridge, J.; Gould, R.W., and Arnone, R.A., 2004. Bottom characterization from hyperspectral image data. *Oceanography,* 17(2), 76–85.

Stumpf, R.P.; Holderied, K., and Sinclair, M., 2003. Determination of water depth with high-resolution satellite imagery over variable bottom types. *Limnology and Oceanography*, 48(1_part_2), 547–556.

U.S. Army Corps of Engineers (USACE), 2009. *Alaska Baseline Erosion Assessment*. Elmendorf Air Force Base, AK: USACE Alaska Study Findings and Technical Report, 68p.

The U.S. Committee on Marine Transportation System (CMTS), 2013. *U.S. Arctic Marine Transportation System: Overview and Priorities for Action*. Washington, DC: CMTS report to the president, 115p.

White House, 2014. *Implementation Plan for The National Strategy for the Arctic Region*. Washington, DC: White House Publication, 32p.